E7e - Magnetic Fields in Coils

Lab Group 6: Jordan Grey([redacted])*(50%)*, [redacted]*(50%)*

November 26, 2024

Abstract

The experimental analysis of magnetic induction $B(z)$ along the z-axis of a long solenoid ($L = 0.348\,\text{m}$) shows minimal variation in the magnetic field at the center, aligning with theoretical predictions. Despite significant relative errors at the solenoid's ends, with a $47.43 \pm 52.00\%$ deviation at the end and a $283.69 \pm 15.80\%$ deviation at the start, most data points fit within the theoretical uncertainty, with $r^2 = 0.8948$. For one coil configuration ($r^2 = 0.9898$), the theoretical z-th for half of the magnetic field is $|z_{th}| = 52.11 \cdot 10^{-3} m$ and experimental $|z_{exp}| = (51.04 \pm 0.5) \cdot 10^{-3} m$. The regions of less than 5% deviation for the Helmholtz coil configuration vary between theoretical and experimental results for different coil separations d. For $d = R/2$, ($r^2 = 0.9856$), the theoretical region spans $z'_{\text{th}} = \pm 15.40\,\text{mm}$, giving a total region of $R_{\text{th}} = 30.80\,\text{mm}$, while the experimental region is $z'_{\text{exp}} = \pm(10.0 \pm 0.5)\,\text{mm}$, resulting in a total region of $R_{\text{exp}} = (20.0 \pm 1.0)\,\text{mm}$. At $d = R$, ($r^2 = 0.9714$), the theoretical region expands to $z'_{\text{th}} = \pm 35.67\,\text{mm}$ with a total of $R_{\text{th}} = 71.34\,\text{mm}$, whereas the experimental region is $z'_{\text{exp}} = \pm(20.0 \pm 0.5)\,\text{mm}$, yielding a total of $R_{\text{exp}} = (40.0 \pm 1.0)\,\text{mm}$. For the largest separation, $d = 2R$, ($r^2 = 0.8160$), the theoretical region is $z'_{\text{th}} = \pm 23.54\,\text{mm}$, totaling $R_{\text{th}} = 47.08\,\text{mm}$, and the experimental region spans $(-10.0 \pm 0.5)\,\text{mm}$ to $+(20.0 \pm 0.5)\,\text{mm}$, giving a total of $R_{\text{exp}} = (30.0 \pm 1.0)\,\text{mm}$.

1 Introduction

This report explores the magnetic field distribution of two main inductive components; the flat coil and the solenoid, with the aim of examining the physical behavior of the magnetic field generated when a constant current I flows through them and comparing measured data with theoretical literature models. For the solenoid, the goal is to compare with theoretical literature along the center axis of the solenoid and examine the behavior of theoretical and experimental results along the end points of the solenoid. The use of flat coils in this report is to examine the behavior of the magnetic field distribution along its center axis for a single and two coils setup. As well as investigated points of interest along the central axis of the coils such as the point of $\frac{1}{2}B_z^{max}$. Additionally, nature of the magnetic induction is examined along the central axis of the Helmholtz coils to, then be compared with theoretical values along the central axis as well as in a region surrounding the setup's central value. Within each section this report is separated into three tasks reflecting the different apparatus and investigations performed to gain a more comprehensive understanding of the nature of a induced magnetic field.

2 Theoretical Basis

2.1 Magnetic field distribution in a solenoid

To examine the magnetic field distribution of a solenoid with a constant DC current through it, with this in mind the magnetic field distribution can be determined through use of the Ampère-Maxwell equation [2]:

$$\oint \vec{H} \cdot d\vec{l} = \iint \vec{j} \cdot d\vec{A} \tag{1}$$

Where:

$$\vec{H} = \text{Magnetic field intensity}(\frac{A}{m})$$
$$\vec{j} = \text{Current Density } (\frac{A}{m^2})$$

Given the use of this Eq. 1 within the scope of the first experimental investigation pertains to solenoids and coils. The solution to Eq.1 obtained under the Bio-Savart Law is [2]:

$$d\vec{H} = \frac{I}{4\pi} \frac{d\vec{l} \times \hat{r}}{|r|^2} \tag{2}$$

Where:

$$I = \text{Current } (A)$$
$$\vec{r} = \text{Position Vector}(m)$$

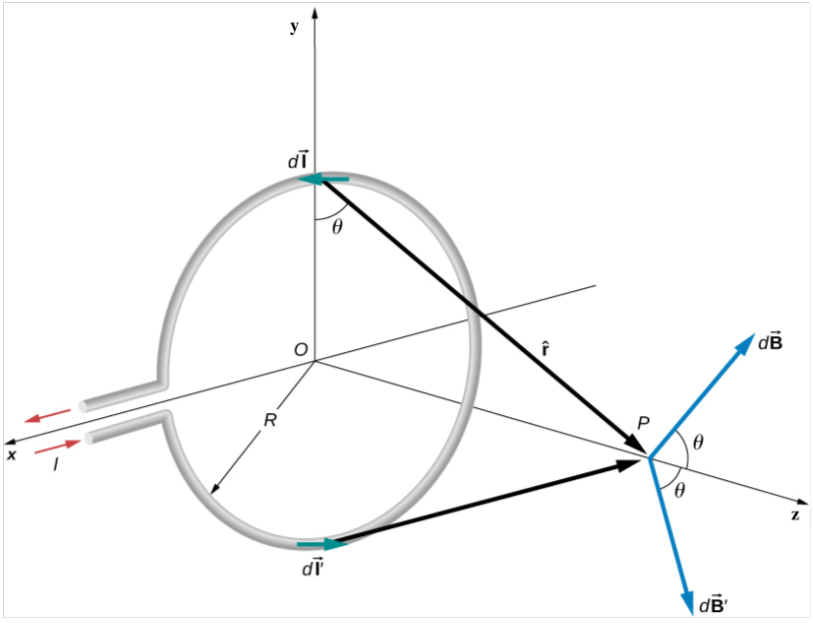

Figure 1: Single loop vector diagram *Source: [1]*

With a lack of a magnetic core the magnetic intensity $\vec{H}$ can be interchanged with the magnetic field $\vec{B}$ through the simple relation:

$$\vec{B} = \mu_0(\vec{H} + \vec{M}), \vec{M} = 0 \implies \vec{B} = \mu_0\vec{H} \tag{3}$$

Where:

$$\vec{B} = \text{Magnetic Field } (T)$$
$$\mu_0 = \text{Permeability of Free Space } (\frac{N}{A^2})$$
$$\vec{M} = \text{Material Magnetization } (\frac{A}{m})$$

The magnetic field distribution in the single loop along the axial line $\hat{z}$ from Fig. 1 and Eqs. 2, 3 is thus given as:

$$dB_z = \frac{\mu_0 I}{2} \frac{1}{(R^2 + (z - z')^2)^{\frac{3}{2}}} \tag{4}$$

Where:

$$B(z) = \text{Magnetic Field along } z \ (T)$$
$$R = \text{Radius of Loop } (m)$$

Eq. 4 is limited to the a single loop, however a solenoid persists over many loops over the total length of the solenoid. to determine the magnetic field as a function of z over the length of a solenoid Eq.4 is manipulated to introduce a turn density coefficient, (n) and the integral with respect to z' is taken over the total length L [3]

$$B(z) = \frac{\mu_0 I n}{2} \left[\frac{z}{\sqrt{R^2 + z^2}} + \frac{L - z}{\sqrt{R^2 + (L - z)^2}} \right] \tag{5}$$

Where:

$$n = \text{Turn density } (\frac{turns}{m})$$
$$L = \text{Length of solenoid } (m)$$

2.2 Magnetic Field in a Flat Coil

For a flat coil with N turns of wire, the law can be applied by summing the contributions of all turns. To calculate the magnetic field along the axis of the loop (not just at the center), the Biot-Savart law gives [3]:

$$B_z = \frac{\mu_0 I R^2}{2(R^2 + z^2)^{3/2}} \tag{6}$$

Where:

$$z = \text{Distance from the center of the loop along its axis}(m)$$
$$R = \text{Radius of the Loop}(m)$$

For a single circular loop of radius R, carrying current I, the magnetic field at the center of the loop (or a point on its axis) is:

$$B = \frac{\mu_0 I}{2R}, \text{ for } z = 0 \tag{7}$$

If the flat coil has N turns, the total magnetic field is approximately N times the field produced by a single loop, assuming the turns are closely packed and lie in the same plane. Thus, the field at the center of the coil becomes [3]:

$$B = N\frac{\mu_0 I}{2R} \tag{8}$$

Where:

$$N = \text{Number of turns}$$

Along the axis, the field is:

$$B_z = \mu_0 I N \frac{R^2}{2(R^2 + z^2)^{3/2}} \tag{9}$$

2.3 Magnetic Field in Two Flat Coils

Using Eq. 9, the magnetic field created by two flat coils can be calculated by adding the fields of the single coils. For Helmholtz configuration, the current direction is the same for both coils, with a distance a between them. The formula of magnetic field at the center point with distance d between the coils is [3]:

$$B = \frac{\mu_0 I N R^2}{2}\left[\frac{1}{[R^2 + (z - \frac{a}{2})^2]^{3/2}} + \frac{1}{[(R^2 + (z + \frac{a}{2})^2]^{3/2}}\right] \tag{10}$$

3 Tasks

3.1 Task I

3.1.1 Experiment Setup

To determine the magnetic induction at the ends of the solenoid, a MR-sensor Adafruit MLX90393 magnetic induction sensor was attached to a plastic rod and mounted to a rider with fixing screws, a solenoid of known $L = 348mm$, $R = 13.1mm$ and $n = \frac{291}{348mm}$ was position beyond the plastic rod as in Fig. 2. The sensor was then placed at a distance of $-60mm$ from the start of the solenoid and a background magnetic induction was recorded for calibration purposes.

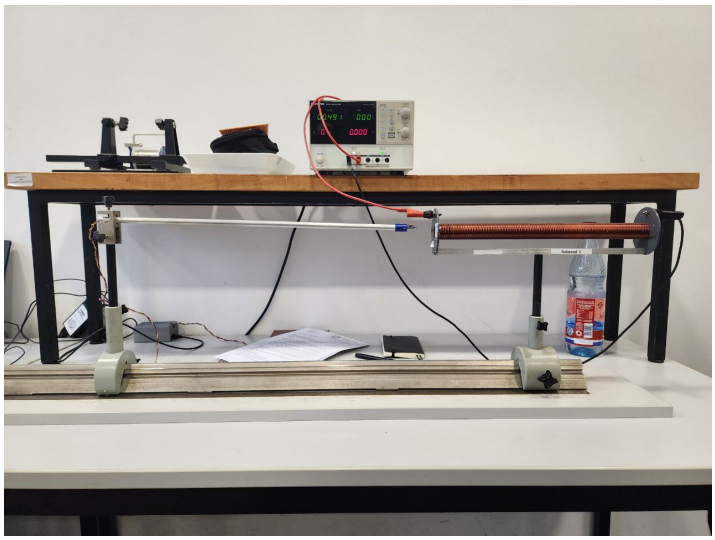

Figure 2: Setup for a solenoid

The laboratory power supply was then set to a steady current of $I = 0.999A$ and supply attached to the solenoid and magnetic induction recorded at a initial position of $-60mm$ to final of $370mm$, *(*$60mm$ *beyond the solenoid)* in $20mm$ increments. These results were then compared to the theoretical results determined by Eq. 5 over the same increments.

3.1.2 Data Analysis

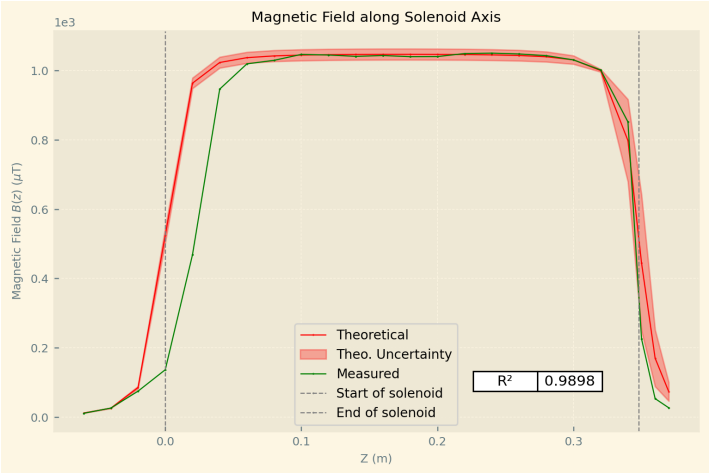

Figure 3: Experimental and Theoretical $B(z)$ along a long solenoid

The results of Fig. 3 shows a similar trend between the measured results and that of the calculated results from Eq. 5 and have an agreement with $r^2 = 0.8948$. Particularly whilst inside the solenoid as all measured points fall within the uncertainty of the calculated results, with exception of two at the beginning. Furthermore the beginning points as the sensor enters the solenoid show the greatest disparity between theoretical results, as they are significantly beyond any degree of uncertainty.

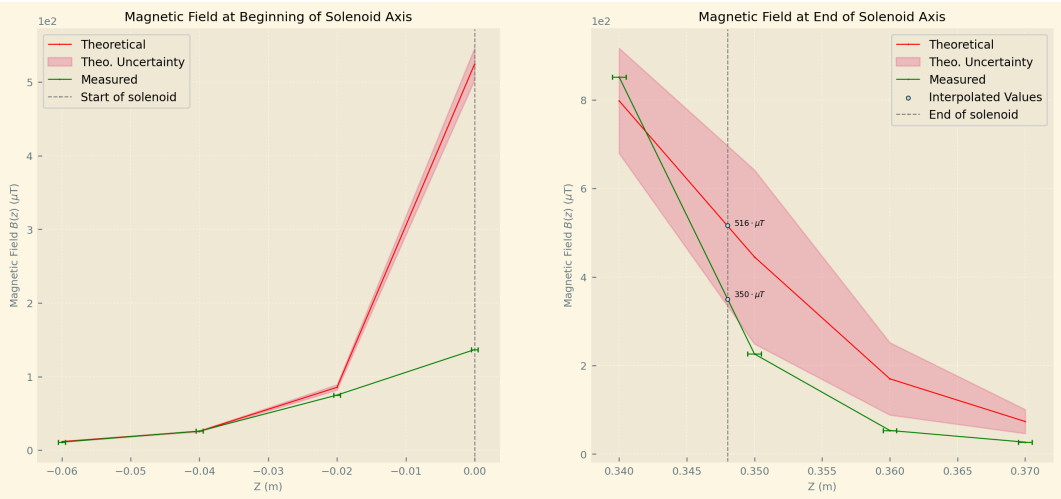

Figure 4: $B(z)$ End points of a long solenoid

Further investigation into the fringe points before and beyond the solenoid, Fig. 4, shows that the measured results are significantly beyond the theoretical results, and it's uncertainty, however follows a similar trend of the theoretical results. It is also noted that interpolation of the data was required the determined the value of the results at the point $z = 0.348m$ as no data at that point was collected.

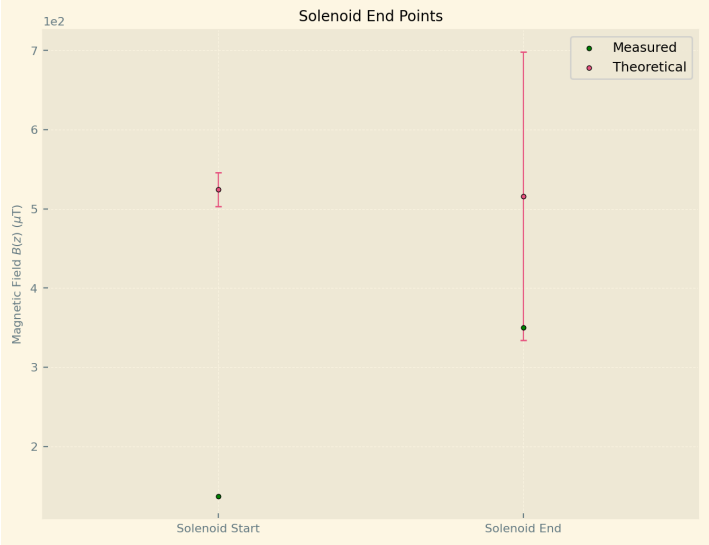

Figure 5: Comparison of end point error

Quantity	**Start**	**End**
Measured Value	$136.7\mu T$	$350.0\mu T$
Calculated Value	$525 \pm 22\mu T$	$(5.2 \pm 1.8) \times 10^2 \mu T$
Absolute Error	$387.81 \pm 21.60\mu T$	$166.00 \pm 182.00\mu T$
Relative Error (%)	$283.69 \pm 15.80\%$	$47.43 \pm 52.00\%$

Table 1: Comparison of Measured and Calculated End Points with Errors

Investigating the end points of the solenoid and comparing theoretical results with measured data, it is clear that the measured value for the start of the solenoid, significantly defers from that of the theoretical results, with a value of $136.7\mu T$ in comparison to the theoretical value of $525 \pm 22\mu T$, and relative error of $283.69 \pm 15.80\%$. The end of the solenoid had a measured result ($350.0\mu T$) that lay inside the uncertainty of the theoretical result with a value of $(5.2 \pm 1.8) \times 10^2 \mu T$, and significantly lower relative error of $47.43 \pm 52.00\%$.

3.2 Task II

3.2.1 Experiment Setup

To measure the magnetic induction using the MLX90393 sensor, the experimental setup begins with fixing the flat coil to a support stand, ensuring that it is oriented horizontally. The coil has N number of turns and a radius R. The power supply is then connected to the coil, placed in series to measure the current I passing through it, as fig. 6 shows. The MLX90393 magnetic field sensor is fixed on a separate support, positioned near the coil at various distances, along the coil's axis to measure the magnetic field strength along coil's center. The sensor is connected to Arduino GUI, which is used to collect and display the magnetic field data. For this setup, the sensor is moved and **not** the coil, collecting measurements of the magnetic field. As the current is constant, the sensor measures the magnetic field at these different positions, providing data that can be used to analyze the relationship between distance from the center of the coil and magnetic field strength at those points.

Initial conditions are:

$$\mu_0 = \text{Permeability of free space} = 4\pi \times 10^{-7} N/A^2$$
$$I = \text{Current through the wire} = (1 \pm 0.0035)A$$
$$R = \text{Radius of the Coil} = 68 \cdot 10^{-3} m$$
$$N = \text{Number of turns} = 320$$

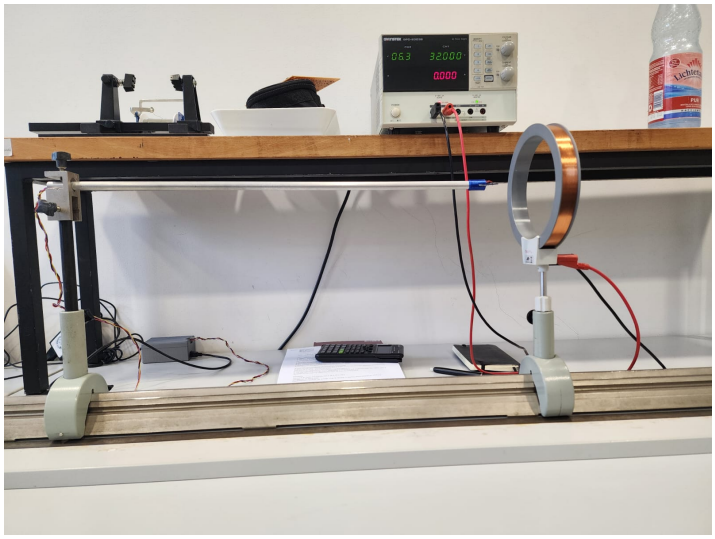

Figure 6: Setup for one Flat Coil

The coordinate system is chosen so it can simplify the analysis as much as possible. The sensor is measuring all the components of the magnetic field of the setup, but the focus is set on y-component corresponding to the z-axis of the coil. The origin is set at the center of the coil, going from -0.1 to 0.1 m on z-axis. The results of this experimental data was then compared with theoretical results determined by Eq. 9.

3.2.2 Data Analysis

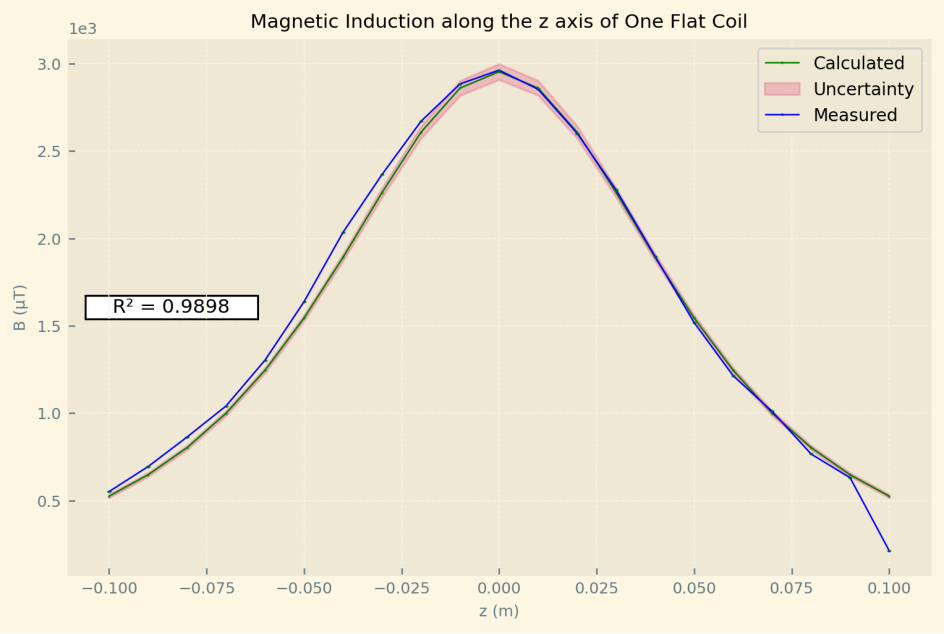

Figure 7: Magnetic Induction of a Flat Coil

Fig. 7 present the graphs of calculated and measured values for magnetic induction along z-axis. Over an interval of 0.2 m the magnetic field is consistent and follows the expected theoretical pattern. The values have an uncertainty that fits most of the measured values and $r^2 = 0.9898$. Both of graph reach maximum at $z = 0$, showing good precision on the choice of coordinate system. For the graph of measured values, an average uncertainty for physical measurements and other factors, such

as precision of the instrument, the environment. It is also of note that the measurement error in z is $\pm 0.25 \cdot 10^{-3} m$. The positions along the z-axis wherein $B(z)$ is half its maximum value were determined to be $|z_{th}| = 52.11 \cdot 10^{-3} m$ and $|z_{exp}| = (51.04 \pm 0.5) \cdot 10^{-3} m$ for the theoretical and experimental results respectively.

3.3 Task III

3.3.1 Experiment Setup

For the next task, the experimental setup begins by mounting two identical flat coils on a support stand, ensuring they are aligned horizontally and positioned symmetrically, as fig. 8 shows. The second coil is added to the previous experimental setup. The coils are arranged so that the distance between their centers is d, with the power supply connected to both coils, in series, to ensure current flow in the same direction. Their half of distance d represents the new origin of the same coordinate system used in the second experiment.

This experiment investigated three different values of $d = \frac{R}{2}$, $d = R$,$d = 2R$ moving the sensor along the z-axis of the two coils from $z = -0.1m$ to $0.1m$ in $0.01m$ intervals. As the current remains constant, the Helmholtz coils setup has the current I **in the same direction**, providing data that can be used to analyze how the magnetic field strength varies with the distance d. The experimental data collected over each value of d, was compared to its respective theoretical values as determined by Eq. 10.

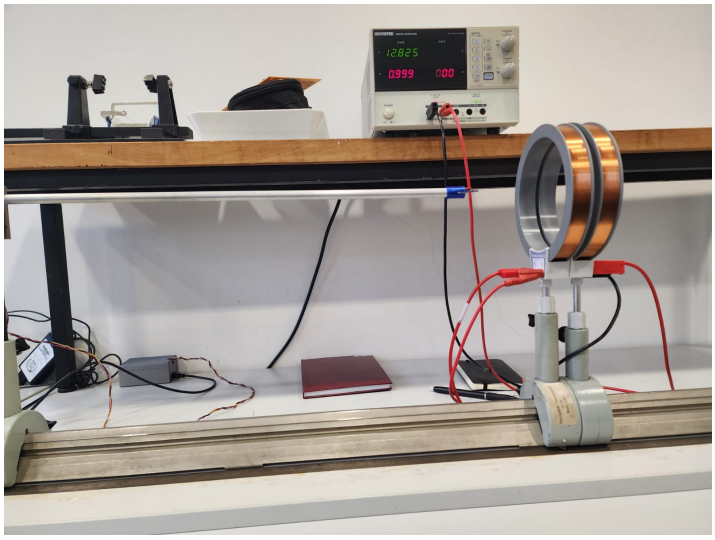

Figure 8: Setup for two Flat Coils at distance D = R/2.

3.3.2 Data Analysis

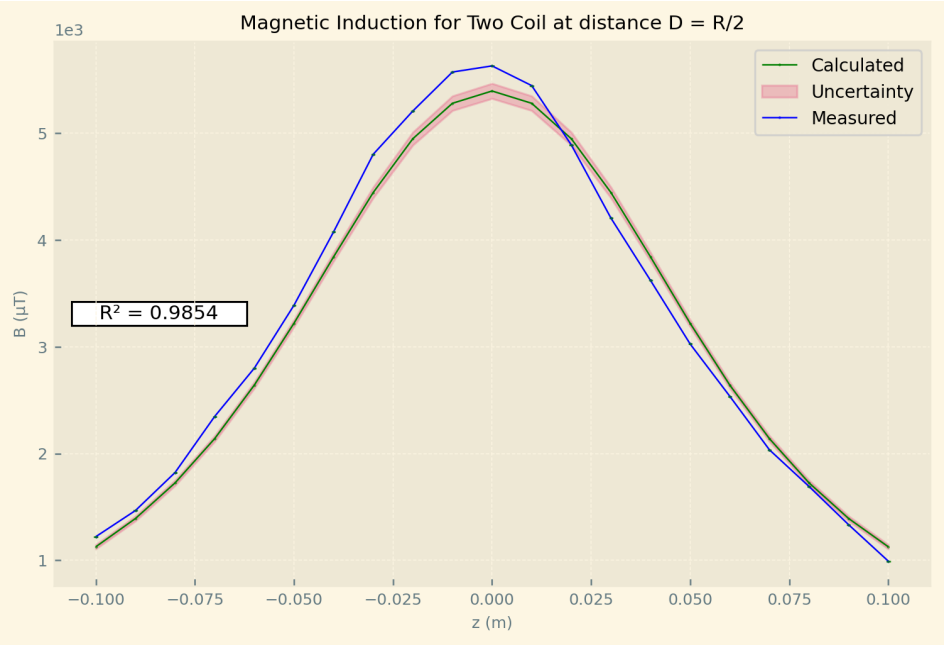

Figure 9: For distance D = R/2

For $d = \frac{R}{2}$, fig. 9 shows the correlations between the measured and calculated data along the z-axis. Over an interval of $0.01m$, slight deviations are observed between the calculated and experimental results. However, the graphs shows $r^2 = 0.9854$, indicating a strong agreement with the theoretical model. The theoretical region with less than 5% deviation is $z'_{th} = \pm 15.40 \cdot 10^{-3} m$, with a total region of $Reg_{th} = 30.80 \cdot 10^{-3} m$ and the experimental is $\pm(10 \pm 0.5) \cdot 10^{-3} m$, with a total region of $Reg_{exp} = (20 \pm 1) \cdot 10^{-3} m$.

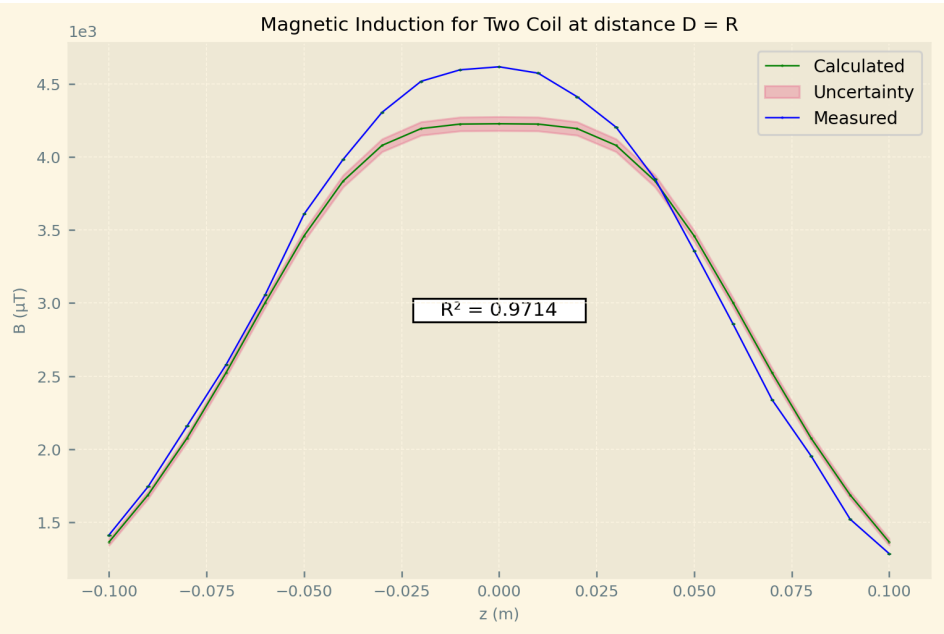

Figure 10: For distance D = R

For $d = R$, fig. 10 displays the correlation between theoretical and measured values, with a $r^2 = 0.9714$,

demonstrating a slightly higher deviation in comparison to $d = \frac{R}{2}$, but still a close fit to theoretical data. The theoretical region with less than 5% deviation is $z'_{th} = \pm 35.67 \cdot 10^{-3} m$, with a total region of $Reg_{th} = 71.34 \cdot 10^{-3} m$ and the experimental is $\pm(20 \pm 0.5) \cdot 10^{-3} m$, with a total region of $Reg_{exp} = (40 \pm 1) \cdot 10^{-3} m$.

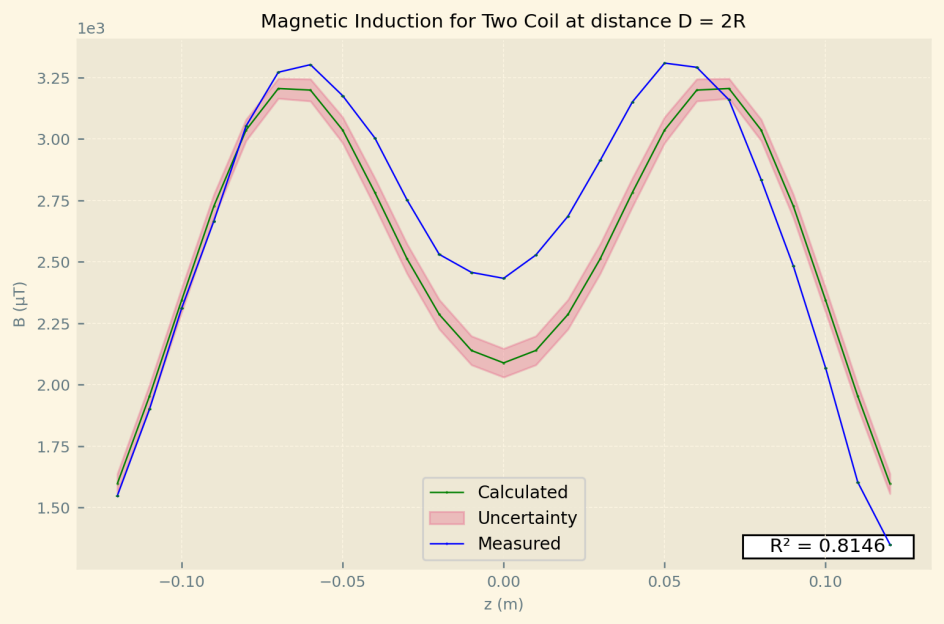

Figure 11: For distance D = 2R

For $d = 2R$, fig. 11 illustrates the measured versus theoretical magnetic field, showing a lower $r^2 = 0.8160$ than either $d = \frac{R}{2}$ or R, reflecting increased discrepancies as the coil separation distance grows. The theoretical region with less than 5% deviation is $z'_{th} = \pm 23.54 \cdot 10^{-3} m$, with a total region of $Reg_{th} = 47.08 \cdot 10^{-3} m$ and the experimental is from $(-10 \pm 0.5) \cdot 10^{-3} m$ to $(20 \pm 0.5) \cdot 10^{-3} m$, with a total region of $Reg_{exp} = (30 \pm 1) \cdot 10^{-3} m$.

4 Discussion

4.1 Task I

The experimental analysis into the magnetic induction $B(z)$ along the z-axis of a long ($L = 0.348m$) solenoid found very little change in the magnetic field inner of the center of the solenoid, which agrees with the theoretical results. Toward the end points of the solenoid, particularly at the beginning of the solenoid the measured data deviates from the theoretical values. It is unknown the exact cause of this significant deviation, it is predicted to be a result of the difference in the point of measurement on the MLX90393 (at it's end point) and the location of sensor on the MLX90393 resulting in a systematic measurement error, wherein the start of the solenoid, indicated on Fig. 3 to truly be more to the right. However it is of note that this systematic error should result the end of the solenoid as indicated truly being more to its right which alters the accuracy of the end of the solenoid. The measured results agree with the theoretical results, with $r^2 = 0.8948$ and this agreement is further enforced with the observation that the large majority of the measured data points collected lie within the theoretical uncertainty.

The outer fringe points outside the solenoid on each side were further investigated Fig.5, up to the entry of the solenoid. It is of note that there is a large disparity between the theoretical values, and its uncertainty, and the measured result. However as the overall trend of both theoretical and measured are alike, and the sharp increase between $z = 0$ and $z = 20mm$. This difference is attributed to the systematic error of the location of the magnetic induction sensor on the MLX90393 accompanied with a comparably small uncertainty in the z-axis. Fig.4 and Table.1 solely compared measured and theoretical results at the start and end of the solenoid. The difference in the measured result and the theoretical value at the end point of the solenoid posses a significant relative error of $(47.43 \pm 52.00)\%$, with a measured result of $350\mu T$ and a theoretical value $(5.2 \pm 1.8) \times 10^2 \mu T$. Although the relative error is significant, the large uncertainty in the calculated value does encompass the measured value and should be noted. It is evident that the difference at the start of the solenoid, is very significant with the measured point having a relative error of $(283.69 \pm 15.80)\%$ with value $136.7\mu T$ in comparison to the theoretical $525 \pm 22\mu T$. It is thus predicted that the systematic error between the measurement point and the sensor location on the MLX90393 is significant and largely impacted the measurement results. Regarding the experimental process conducted in this experiment, only 24 data points were collected over the span of $.430m$ as such for future study it is recommended two increase the data point collected to undoubtedly increase the resolution of data and thus significance of findings. Also recommended is to assess MLX90393 for the location of the sensor and use this point and the reference point for the sensor to more accurately record the $B(z)$ along solenoid's axis.

4.2 Task II

For the second task, the experimental setup and the measurements provide valuable information about the relationship between the magnetic field and distance from the center of the coil.
As the Fig.7 is analyzed, the difference between the calculated and measured values mostly fits the experimental uncertainty. The graphs capture a coefficient of determination of $r^2 = 0.9898$, indicating a close fit to the expected data.
Although, when analyzing the distance from the central value to the half of the magnetic fields magnitude, the majority of the measured values fall between the uncertainty of the calculated values. However, not all the values fit the uncertainty, suggesting that there might be systematic errors in the experimental setup or some unaccounted environmental factors, such as stray magnetic fields (from other electronic devices) or temperature fluctuations were not considered. The magnetic field of the Earth was substracted from the beginning of the computation. The magnetic field is symmetric about $z = 0$, with both theoretical and experimental graphs peaking at this point. This confirms a proper alignment of the coil and sensor in the chosen coordinate system, as well as the expected behavior of the magnetic field along the axis of a circular coil.

4.3 Task III

For the third task, the correlation between the theoretical and experimental magnetic field measurements for coils separation distance, d, highlights the model's reliability and its limitations. Each case presents unique characteristics, with deviations increasing as d grows.

For $d = R/2$, the graph is the similar to the graph for one coil, but double in magnitude for the values, indicating that the setup works a lot like a single coil with longer length. This is an ideal setup for seeing the key features and advantages of the Helmholtz configuration. The $r^2 = 0.98564$ is indicating a strong agreement with the theoretical values. The theoretical region with less than 5% deviation is $z'_{th} = \pm 15.40 \cdot 10^{-3} m$, corresponding to a total region $Reg_{th} = 30.80 \cdot 10^{-3} m$ and the experimental is $\pm(10 \pm 0.5) \cdot 10^{-3} m$, giving a total experimental range of $Reg_{exp} = (20 \pm 1) \cdot 10^{-3} m$. The proximity of these regions reflects the strong predictive power of the theoretical model for small coil separations. Any discrepancies are likely due to systematic factors, such as minor wrong alignments in the experimental setup or environmental noise.

In fig. 10, the correlation between theoretical and measured values for $d = R$ displays a slightly higher deviation compared to $d = R/2$. The $r^2 = 0.9714$, though slightly lower than that of $d = \frac{R}{2}$, still demonstrates a strong alignment between the data and the model. The theoretical region with less than 5% deviation is $z'_{th} = \pm 35.67 \cdot 10^{-3} m$, with a total region of $Reg_{th} = 71.34 \cdot 10^{-3} m$ and the experimental is $\pm(20 \pm 0.5) \cdot 10^{-3} m$, with a total region of $Reg_{exp} = (40 \pm 1) \cdot 10^{-3} m$.

The last chosen distance is $d = 2R$, the largest coil separation in this report, with $r^2 = 0.8160$, indicating a noticeable drop in the measured accuracy to the theoretical values. The theoretical region with less than 5% deviation is $z'_{th} = \pm 23.54 \cdot 10^{-3} m$, with a total region of $Reg_{th} = 47.08 \cdot 10^{-3} m$ and the experimental is from $(-10 \pm 0.5) \cdot 10^{-3} m$ to $(20 \pm 0.5) \cdot 10^{-3} m$, with a total region of $Reg_{exp} = (30 \pm 1) \cdot 10^{-3} m$.

These results collectively suggest that the accuracy of the Helmholtz configuration diminishes as d deviates further from the ideal configuration, $d = R/2$. The significant decrease in experimental data with the theoretical model indicates that as the coil separation increases, the model's assumptions may no longer explain the physical system's behavior.

With larger coil separations, the magnetic field becomes weaker and less consistent across the z-axis. The field's intensity decreases, leading to greater deviations between calculated and measured values. The regions of agreement (both in the 5% deviation range and in terms of r^2) shrink as d increases. This reflects how the uniformity of the magnetic field diminishes as the coils are separated.

References

[1] Magnetic Field of a Current Loop. https://phys.libretexts.org/@go/page/4424, July, 9 2024. [Accessed: 2024-11-22].

[2] D. J. Griffiths. *Introduction to Electrodynamics*. Pearson, 4th edition, 2013.

[3] M. Ziese. *E07e Magnetic Fields in Coils*. Universität Leipzig, November 2024.